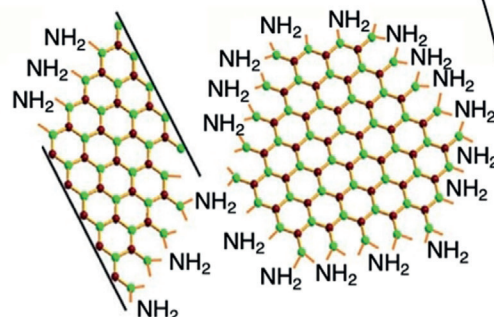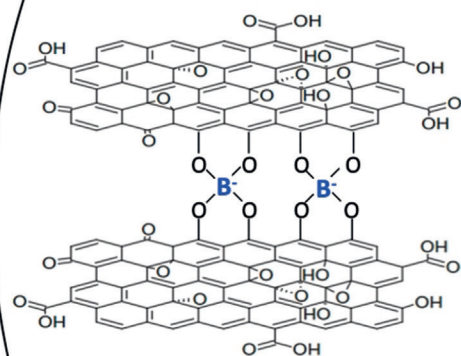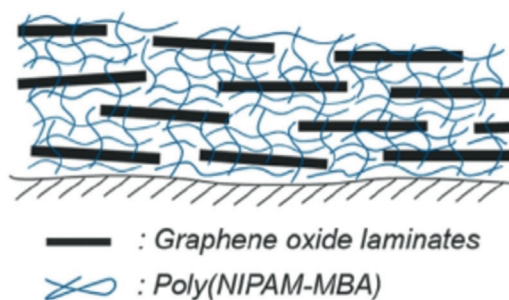# 2D Nanosheets and Their Composite Membranes for Water, Gas, and Ion Separation

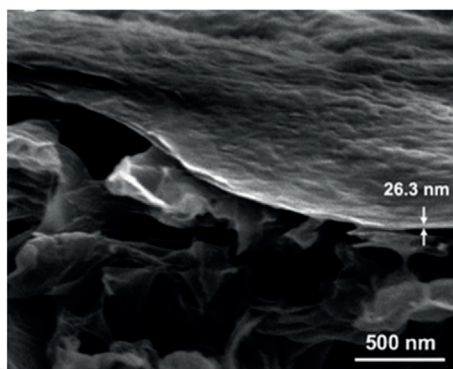*Seungju Kim, Huanting Wang, and Young Moo Lee**

: Graphene oxide laminates

: Poly(NIPAM-MBA)

2D Nanocomposite Membranes

26.3 nm

500 nm

*T*wo-dimensional nanosheets have shown great potential for separation applications because of their exceptional molecular transport properties. Nanosheet materials such as graphene oxides, metal–organic frameworks, and covalent organic frameworks display unique, precise, and fast molecular transport through nanopores and/or nanochannels. However, the dimensional instability of nanosheets in harsh environments diminishes the membrane performance and hinders their long-term operation in various applications such as gas separation, water desalination, and ion separation. Recent progress in nanosheet membranes has included modification by crosslinking and functionalization that has improved the stability of the membranes, their separation functionality, and the scalability of membrane formation while the membranes' excellent molecular transport properties are retained. These improvements have enhanced the potential of nanosheet membranes in practical applications such as separation processes.*

1. Introduction

Membrane-based separation processes are a widely applied and continuously developing technique. Due to their high energy efficiency, membrane-based separation processes have become a possible alternative to energy-intensive, traditional separation processes. The recovery of a valuable component from a mixture is possible by a membrane process without additional energy or chemical cost. Various membrane-based separation applications, such as gas separation, water and liquid purification by microfiltration, ultrafiltration, nanofiltration, and reverse osmosis (RO) desalination, energy production by pressure-retarded osmosis and fuel cell applications, and electrodialysis have been successfully applied for industrial-scale operations during the last few decades.[1]

Water processing by salt and ion separation and gas separation applications are successfully industrialized membrane-based technologies. Membrane-based water and liquid treatment has played an important role in the reclamation of wastewater, production of potable water, and the purification of valuable components, and has been applied in various areas such as pharmaceuticals, manufacturing, and mining industries. Significantly, the RO process is the most widely applied water desalination technology due to its low cost and energy consumption. The RO process for seawater desalination produces 65% of all the drinkable water worldwide.[2] Recent water scarcity issues have drawn attention to the RO process as a major water production technology. Ion separation membranes, cation exchange membranes, and anion exchange membranes use an electrical potential difference by application of an electric field to force ions to pass from the feed side to the receiving side. Ion exchange membranes separate monovalent and/or multivalent ions to remove salts or ions from feed liquids such as brackish water, seawater, glycol, and glycerine. Since membrane-based gas separation processes have a very small carbon footprint and low energy consumption, these processes can be much smaller than other technologies. With these advantages, membrane-based gas separation applications have been used for many compact processes such as offshore gas separation plants, natural gas production and purification, and removal of volatile fumes in airplane fuel tanks. Gas production applications such as hydrogen production, air separation for nitrogen production and oxygen enrichment, carbon dioxide (CO_2) separation for natural gas purification, and olefin/paraffin separation have been a main target for membrane gas separation technology. More recently, environmental problems such as global warming by greenhouse gases have pointed to membrane-based separation as a means to remove and sequester CO_2 from industrial sources.

Polymer-based membranes have dominated the membrane market. Polymers can be dissolved in organic solvents or melted into a liquid form that can be fabricated into various membrane types such as thin film composites and hollow fibre membranes for module preparation. Commercial polymers such as polysulfone, polyimide (PI), polyamide (PA), cellulose acetate (CA), and poly(vinylidene fluoride) have been used for membrane applications in industry. However, the less effective molecular transport and separation performance of polymer membranes due to their small pore size and broad pore size distributions hinders the overall efficiency of polymer-based membrane processes. Owing to the chemical and thermal degradation of polymer materials under harsh operating conditions, additional pretreatment processes are needed to ensure long-term operational stability. Some rigid and microporous polymers, such as thermally rearranged polymers and polymers with intrinsic microporosity, exhibited a high gas permeability and selectivity for gas separation applications.[3] However, there is still a need for high performance, polymer membrane materials.

Recently developed, two-dimensional (2D) nanosheet materials, such as metal–organic frameworks (MOFs),[4]

[*] Dr. S. Kim, Prof. Y. M. Lee
Department of Energy Engineering, Hanyang University
Seoul 04763 (Republic of Korea)
E-mail: ymlee@hanyang.ac.kr

Prof. H. Wang
Department of Chemical Engineering, Monash University
Clayton, Victoria 3800 (Australia)

(iD) The ORCID identification number(s) for the author(s) of this article can be found under:
https://doi.org/10.1002/anie.201814349.

covalent organic frameworks (COFs),[5] and graphene oxide (GO),[6] have been considered as attractive building blocks to construct high-performance separation membranes (Figure 1) because of their atomic thickness, robustness, and potential for functionalization. The precise and fast molecular transport properties of 2D nanosheet membranes come from their intrinsic nanopores in the nanosheets as well as their nanochannels between stacked nanosheets. Graphene-based membranes are the most widely studied nanosheet membranes and include porous graphene, graphene oxide (GO), and reduced graphene oxide (rGO).[6] Among them, GO membranes have demonstrated unique molecular transport properties caused by hydroxyl groups on GO, which provide nanochannels suitable for the transport of ions and small molecules. GO membranes are usually prepared by coating methods such as spin-coating or filtration, which form ultrathin GO layers on a porous supporting layer with excellent mechanical stability. GO-based membranes are promising membrane materials that can be prepared with large effective areas. The remarkable molecular transport and separation properties of GO membranes can improve the efficiency of an entire process by increasing productivity and product purity. However, because these hydroxyl groups on the GO membranes interact with water molecules, the membranes are likely to lose dimensional stability in aqueous environments. In water treatment applications, despite GO's high water permeability, the relatively low salt rejection ability of GO membranes for monovalent ions, for example, NaCl, has diminished its application in water desalination. Other 2D nanosheet membranes showed similar dimensional instability or low performance, which has hindered their use in practical applications that require long-term performance stability. 2D nanosheet membranes need additional improvements before commercialization.

Recently developed nanosheets and their composite membranes have enhanced stability and more possibilities for practical applications. The modification of 2D materials has improved the overall materials properties for membrane

Dr. Seungju Kim received his PhD in 2014 in Energy Engineering from Hanyang University in the area of membrane fabrication for carbon dioxide separation. From 2015 to 2017 he was a postdoctoral fellow in Chemical Engineering at Monash University. His current research interests include the development of membrane materials such as polymers, graphene, and metal–organic frameworks for membrane separation applications.

Huanting Wang is a Professor in the Department of Chemical Engineering at Monash University, Australia. He received his PhD in materials science and engineering from the University of Science and Technology of China in 1997, and conducted postdoctoral research at the California Institute of Technology and University of California Riverside. His current research focuses on the development of nanostructured materials and membranes for gas separation, fuel cells, and water treatment.

Young Moo Lee is Hanyang Distinguished Professor of Energy Engineering and also served as President at Hanyang University. He received his BS and MS degrees at Hanyang University, and his PhD in fiber and polymer science at North Carolina State University in 1985. He is interested in membrane materials and processes for gas and vapor separation including thermally rearranged polymer materials, organic–inorganic hybrid membranes, surface-modified membranes, and biomaterials.

processes, solving the problems of previously developed 2D membranes. The modifications, such as chemical and physical crosslinking, functionalization, and inclusion in polymer nanocomposites, tightly bind the 2D nanosheets, which controls the space between nanosheets and its effects on molecular transport properties, and also increases dimensional stability. Various crosslinkers, such as linear and aromatic monomers with amide bonds, or polymers that physically entwine nanosheets with polymer chains, have been incorporated into 2D materials to build ultrathin nanocomposite membranes. After the development of graphene materials, numerous graphene-like 2D materials have been investigated and widely reviewed in the articles dealing with their physiochemical properties, fabrication approaches, and applications.[7] Synthetic methodologies in solution-based methods for constructing layered structures and exfoliating 2D materials under relatively mild conditions were developed, resulting in uniformly sized, high-quality, and single- or few-layered nanosheets. 2D
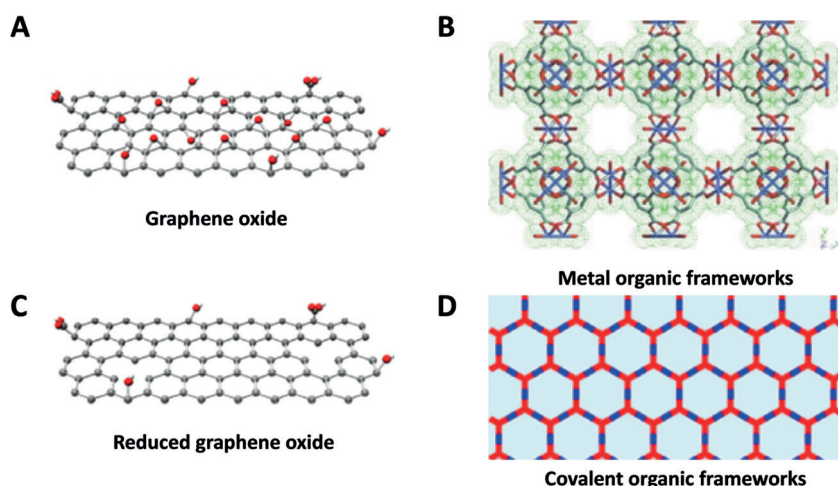
Figure 1. Examples of 2D materials. A) Graphene oxide,[6] B) metal–organic frameworks,[4] C) reduced graphene oxide,[6] D) covalent organic frameworks.[5] Copyright 2015, Elsevier. Copyright 1999, The American Association for the Advancement of Science. Copyright 2013, American Chemical Society.

materials have shown great potential in applications such as electronic and optical devices, sensors, catalysis, and energy storage,[7a–c] but they still present some issues as membranes for practical separation processes.[7d–g] More recent studies demonstrated 2D nanocomposite membranes that would open the door for 2D materials to be applied in membrane-based separation applications and become promising alternatives to current polymer-based membranes. This Minireview will provide the latest information on polymer nanocomposites and modified nanosheet membranes, including their fabrication methods and performance in membrane applications. Specially, we focus on membrane fabrication beyond fundamental levels for large-scale applications that could be achieved by modification of the state-of-the-art 2D materials. Current challenges of 2D membranes for material synthesis and up-scaling are also addressed.

2. Formation of 2D Nanosheets and Their Composite Membranes
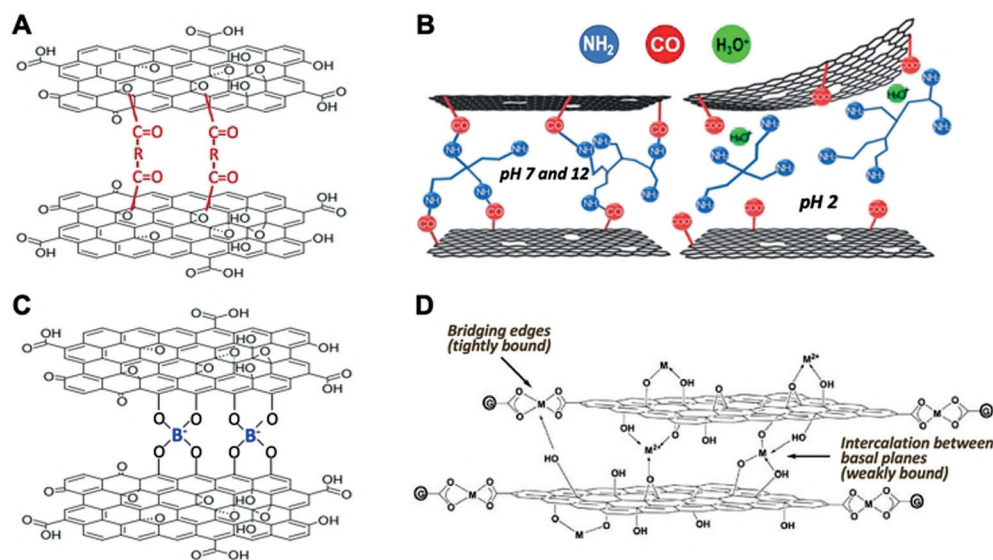
2.1. Graphene-Based Materials

Graphene-based materials, such as porous graphene, GO, and rGO, are among the first developed examples of 2D membranes. From the porous graphene membranes prepared by oxidative etching or nitrogen functionalization to the latest rGO membranes obtained by post-reduction of GO after formation of a membrane layer, graphene-based membranes have exhibited a potential for gas, water, and ion separation applications. Graphene-based membranes have been introduced to other polymer-based membranes to give enhanced properties such as processability and anti-fouling capabilities. Most of the membranes are prepared on a porous substrate as a thin-film composite. Facile preparation methods such as vacuum filtration and spin-coating for the fabrication of membranes with large areas also brought the possibility of graphene-based membranes for industrial applications. However, for application in gas separation and water treatment, which are the most widely applied membrane processes, graphene-based membranes are currently inappropriate because of their low separation efficiency and performance instability for long-term membrane operation. To overcome these drawbacks, the modification of GO by crosslinking has been widely studied. Hydroxyl and carboxyl groups on GO are the main groups that are used to functionalize GO be-

cause of their high reactivity. The amount of hydroxyl and carboxyl groups on GO can be controlled during GO preparation.

Covalent crosslinking by esterification or amidation via a coupling reaction with small molecules or polymers is a facile modification method that controls the stability of GO nanosheets and the molecular transport properties of GO membranes.[8] Crosslinked GO was developed as a layered material to improve its mechanical properties such as strength, stiffness, and toughness. GO-based layered composite materials including GO-poly(vinyl alcohol),[9] GO-poly-(methyl methacrylate),[10] GO-borate,[11] and GO-polydopamine,[12] were fabricated by crosslinking after formation of a GO layer. These studies focused on the mechanical properties of the GO materials and showed that the integration improved the connectivity of the GO nanosheets, which led to an increase in both tensile strength and toughness. Covalent crosslinking by esterification using dicarboxylic acids could control the physical properties of the nanosheet membranes (Figure 2a).[13] The use of various crosslinkers such as ethylene glycol, propandioic acid (PA), glycerol, and neopentyl glycol with different chain lengths can adjust the interlayer spacing and elastic moduli and lead to advances in precise molecular separation. The interlayer spacing of pristine GO is about 0.69 nm but is increased to 6–7 nm in the aqueous state due to its high swelling tendency.[14] Covalent crosslinking through crosslinkers containing hydroxyl groups resulted in a regular interspacing of 0.76 nm, with less swelling tendency, depending on the type of crosslinker. The crosslinking of GO nanosheets also increased the elastic moduli from 0.03 to 3.49 GPa.[13]

Amidation is another method for chemically crosslinking GO that is also widely used for PA preparation.[15] Nam et al. introduced a polycarbonate (PC) support functionalized with branched polyethylenimine (BPEI) and GO nanosheets for a crosslinking reaction (Figure 2b).[15a] After BPEI had been

Figure 2. Crosslinking of graphene-based materials by A) esterification,[13] B) amidation,[15a] C) borate crosslinking,[18] D) metal ion crosslinking.[19a] Copyright 2008, 2016, American Chemical Society. Copyright 2017, Elsevier.

coated on a porous PC support by immersion in a commercial BPEI solution, a GO solution was filtered to form a GO layer, and carboxyl groups on the GO were crosslinked with amine groups of BPEI. This method avoided excessive intercalation and retained the same interlayer spacing of GO, but greatly improved the dimensional stability over a broad pH range. The resulting composite membranes strongly attached to the polymer support and bonded with other GO nanosheets, improving stability in both acidic (pH 2) and basic (pH 12) aqueous solutions. However, the GO composite membrane still detached in acidic solution when sonicated because the amide bonds in the crosslinking region were partially converted into amine and carboxylic acid groups. The conversion was attributed to hydrolysis in the presence of protonated ions and the weakened π–π interactions between GO nanosheets under acidic conditions.

Borate crosslinking is one of bio-inspired methods taken from higher-order plants in which borate reinforces the intercellular structure via crosslinking of polysaccharide rhamnogalacturonan II to build stiffened and strong cell walls.[11,16] This method is applied by co-filtration or separated filtration of an aqueous dispersion of GO and sodium tetraborate followed by annealing at low to medium temperature. Borate crosslinking also forms covalent bonds with oxygen-containing hydroxyl groups in GO and increases the film stiffness and strength nearly 80% over that of an untreated film. The use of different types of boronic acids as crosslinkers changed the interlayer spacing from 0.75 to 1.05 nm, which led to improved hydrogen (H_2) and CO_2 uptake capacity. Song et al. also used borate crosslinking, inspired by natural nacre, to create supertough (toughness of 15.3 $MJ\,m^{-3}$) artificial nacre that consisted of stacked GO nanosheets with π–π interactions and hydrogel bonding.[17] A similar approach to form a GO composite membrane on a tubular polymer membrane surface was made with a vacuum-assisted preparation method (Figure 2c).[18] Nanochannels were engineered by manipulating the annealing process and the chemistry of the boron bridges; this affected the molecular transport properties through the membrane. These studies demonstrated the use of GOs as building blocks for nanoporous materials.

Chemical interactions between functional groups on GO and divalent metal ions enhance the mechanical properties of GO nanosheets.[19] While a GO dispersion remains stable in the presence of monovalent metal salts such as LiCl and NaCl, the addition of divalent alkaline salts such as $MgCl_2$ and $CaCl_2$ leads to the agglomeration of GO nanosheets by crosslinking. Park et al. employed this crosslinking method with unmodified GO paper made by filtration on an anodisc membrane filter. Aqueous $MgCl_2$ or $CaCl_2$ was added to the GO paper to activate the crosslinking reaction (Figure 2d).[19a] This modified GO nanosheet had more tightly bound bridging edges between GO nanosheets (*x*-direction crosslinking) and less tightly bound intercalation between the basal planes (*y*-direction crosslinking). The small amount of divalent metal ions (less than 1 wt%) enhanced the modulus and tensile strength of the GO paper through simple chemical modification, and these graphene-based materials were applied for macroscale structures. Mono- and divalent metal

cations (K^+, Na^+, Ca^{2+}, Li^+, Mg^{2+}) are capable of fixing the interlayer spacing of GO nanosheets between 1.14 and 1.36 nm, but a mixture of salts, that is, KCl + M (M = NaCl, $CaCl_2$, LiCl, or $MgCl_2$) could reduce the interlayer spacing down to 1.12 nm with a high precision of 0.1 nm that remained stable over 140 h.[19b] This suggested that GO membranes with the precisely tuned interlayer spacing could present precise molecular separation. Yeh et al. also found a similar result by crosslinking with divalent or trivalent metal ions and showed that GO nanosheets prepared on a porous anodized aluminum oxide (AAO) disc had better stability in water than GO nanosheets prepared on Teflon film due to the existence of Al^{3+} ions.[19c] AAO filter discs, which are very common supports for membrane preparation, especially for 2D materials, are likely to corrode and release Al^{3+} ions during filtration of an acidic GO dispersion. Other divalent ions such as Mn^{2+} ions, which are one of by-products during GO synthesis by chemical methods, can also crosslink GO nanosheets and improve the mechanical properties of GO membranes. It was confirmed by additional experiments that GO nanosheets modified by other divalent ions, such as Zn^{2+}, Ca^{2+}, Mg^{2+}, and Ni^{2+}, have increased intrinsic mechanical properties due to the formation of water-stable and less-swollen GO membranes.

The development of scalable processes for membrane fabrication is essential for propelling these outstanding membrane materials into industrial applications. Ultrathin GO membranes on a supporting layer are conventionally prepared by vacuum-assisted filtration or spin-coating methods; this approach is suitable for lab-scale membrane fabrication. However, some approaches for fabricating graphene-based membranes have been reported using casting or spray-coating, methods appropriate for membrane manufacturing (Figure 3). Akbari et al. prepared highly ordered thin films of multilayered GO by a shear-alignment approach.[20] Viscoelastic GO ink, which was concentrated from a GO aqueous dispersion by the addition of hydrogel beads, was cast on a polymer substrate such that the nematic phase of GO was aligned forming a highly ordered layer. This method formed a GO layer with a thickness of 150 nm for nanofiltration applications but can be modified by reducing the layer thickness. Morelos-Gomez et al. reported the preparation of a hybrid layer of GO and few-layered graphene (FLG) with deoxycholate (DOC) by spray-coating an aqueous dispersion.[21] A GO/FLG layer with a thickness of 26–33 nm was formed on the poly(vinyl alcohol) (PVA)-coated polysulfone substrate, followed by thermal treatment at 100 °C and Ca^{2+} crosslinking with $CaCl_2$ solution; the resulting hybrid layer endured high-pressure water treatment at 50 bar. The spray-coating deposition method is scalable and environmentally friendly and can be applied for other 2D membranes.

In GO–polymer nanocomposites interactions also exist between the functional groups on GO and the polymer. Network polymers, such as hydrogels, have been used to integrate GO nanosheets into the polymer phase. Two main strategies have been developed for the preparation of GO–hydrogel nanocomposites: in situ polymerization of water-soluble monomers in a GO dispersion, and simple mixing of
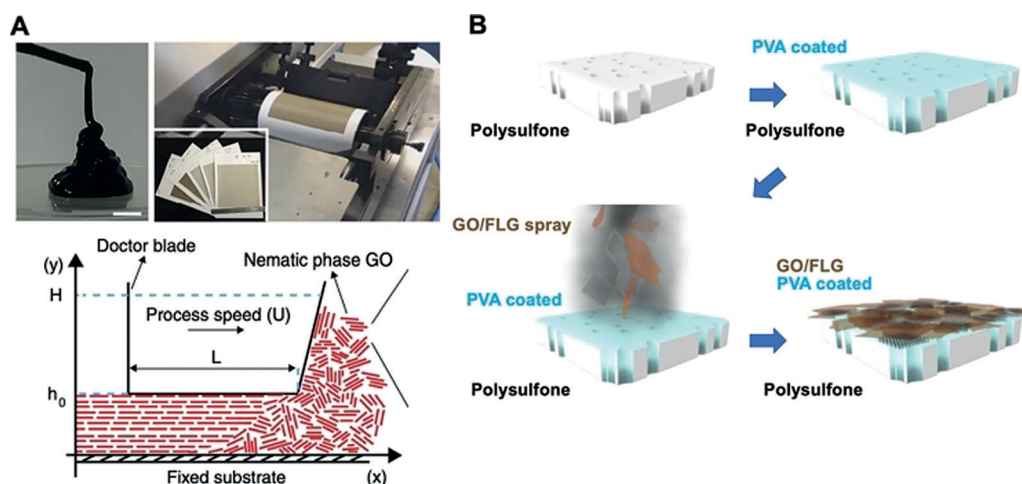
Figure 3. A) Fabrication of shear-aligned membrane from nematic GO ink.[20] B) GO/FLG membrane preparation on porous substrate by spray-coating.[21] Copyright 2016, 2017, Springer Nature.

GO and a hydrogel in solution.[22] Various hydrogels, such as poly(acrylic acid) (PAA), PVA, polyacrylamide, and poly(N-isopropylacrylamide) (PNIPAM) with the crosslinker *N,N′*-methylenebis(acrylamide) (MBA), have been introduced to prepare GO–polymer nanocomposites. Kim et al. incorporated GO with poly(NIPAM-MBA), which is a highly crosslinked hydrogel (Figure 4).[22c] An aqueous solution containing GO nanosheets and monomers was spin-coated on a porous substrate and then polymerized by free radical polymerization initiated under heat treatment with a catalyst. GO nanosheets were crosslinked with the polymer phase without chemical bonds but only bound by poly(NIPAM-MBA), which prevented swelling of the membrane in water. GO nanosheets were also applied as a scaffold for the fabrication of ultrathin membranes because of the intrinsic 2D nature of GO. Moreover, GO crosslinking resulted in significant improvements in the dimensional stability of the membrane in that it was not delaminated during a desalination operation. Zhong et al. prepared GO and PAA hydrogel nanocomposites by in situ free radical polymerization with an ammonium persulfate catalyst (Figure 5).[22b] Ferric nitrate was also introduced so that Fe^{3+} ions could influence the crosslinking of the GO nanosheets. The free radical polymerization was very rapid and the GO nanosheets were trapped

in the polymer network. Because PAA hydrogel is an elastic material, the GO–PAA composites showed outstanding toughness and stretchability. In this case, a small amount of GO (0.5 wt%) and Fe^{3+} ions (0.5 wt%) were employed, into the hydrogel phase, but the mechanical properties of the resulting hydrogel composite greatly improved, with a tensile strength of 777 kPa, elongation at break of 2980%, and work of extension of 11.9 MJ m^{-3}. This also showed the potential for medical uses: owing to the great self-healing property of the composite, it can automatically heal damage without an external stimulus. Bai et al. introduced PVA hydrogel as a physical crosslinking agent for a nanocomposite that was formed by the assembly of GO nanosheets and crosslinked PVA.[22a] Hydroxyl groups on both GO and PVA enhanced the interfacial interaction and the mixture immediately formed a gel. The GO–hydrogel composite was pH-sensitive, formed a gel under acidic conditions, and underwent a gel–sol transition under alkaline conditions.

2.2. 2D Metal–Organic Framework Materials

Metal–organic frameworks (MOFs) are intrinsically porous materials consisting of metal ions linked by organic
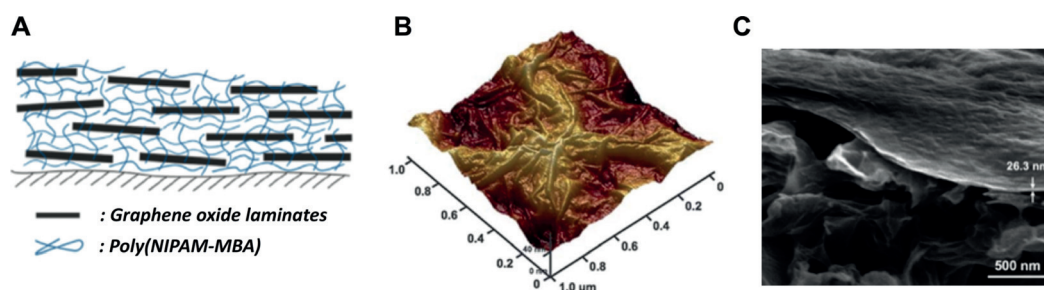
Figure 4. GO crosslinking by network poly(NIPAM-MBA).[23] A) Schematic image of GO–polymer nanocomposite. B) Surface AFM image.[22c] C) Cross-sectional SEM image of GO–polymer membrane on nylon substrate.[22c] Copyright 2018, Elsevier. Reproduced by permission of The Royal Society of Chemistry, 2017.
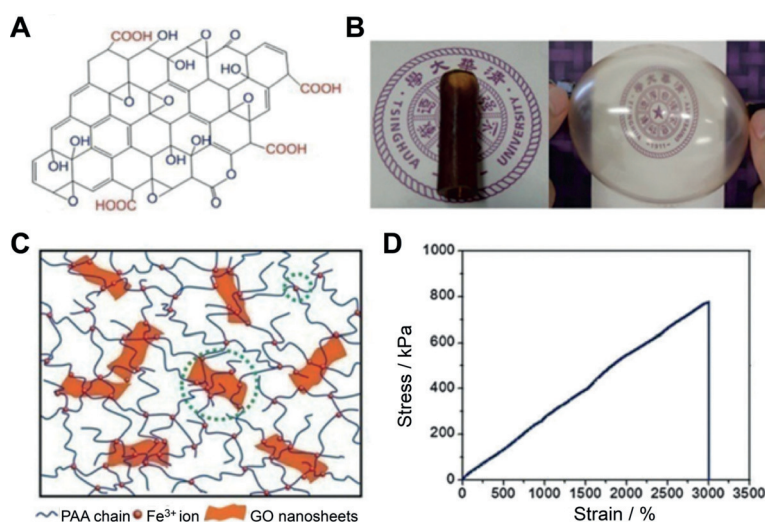
Figure 5. GO crosslinking by poly(acrylic acid).[22b] A) The chemical structure of GO., B) A GO–PAA nanocomposite hydrogel tube (left) blown into a balloon (right), indicating its outstanding toughness and stretchability. C) Scheme of the three-dimensional network structure of GO–PAA nanocomposite hydrogels facilitated by Fe^{3+} ions with dual cross-linking effects (the smaller green dotted circle represents the first cross-linking points that are Fe^{3+} ions creating ionic cross-links between PAA chains, and the larger green dotted circle represents the second cross-linking points where GO nanosheets link PAA chains through coordination). D) Stress–strain curve of GO–PAA nanocomposite hydrogels. Reproduced by permission of The Royal Society of Chemistry, 2015.

bridging ligands that usually form crystalline compounds. Since their discovery, more than 20 000 different MOFs have been reported with large surface areas, ranging between 1000 to 10 000 $m^2 g^{-1}$, and well-ordered pore structures, with applications in, for example, catalytic transformations, gas adsorption, and proton-conducting membranes.[24] Because of their highly ordered structure and strong chemical bonds, MOFs are three-dimensional (3D) crystals when prepared without dimensional controls.[25] However, for use in membrane-based separation processes, fabrication methods for thin MOF layers have been investigated because membrane thickness is an important parameter to improve molecular transport properties. For example, the secondary growth method of zeolitic imidazolate frameworks (ZIFs) was introduced to effectively control and orientate ZIF crystals on a substrate, and a defect-free thin layer of ZIFs with a controlled thickness was synthesized.[26] Some other approaches to form MOF nanosheets were developed by using 2D ligands as linkers.

Layered MOFs prepared by stacking 2D MOF layers, with relatively weak hydrogen-bonding interactions or π–π interactions between planar organic molecules, are known to be easily exfoliated into nanosheets by mechanical processing, sonication, or chemical exfoliation.[27] Peng et al. applied a mechanical exfoliation method to layered $Zn_2(bim)_3$ and

$Zn_2(bim)_4$ precursors (bim = benzimidazole) by ball milling. This resulted in MOF nanosheets with sub-10 nm thickness and 0.29 nm honeycomb-like pores.[28] Because physical exfoliation might damage the structure of MOFs, ball milling at a very low speed of 60 rpm followed by ultrasonication in a volatile solvent facilitated the formation of single-layer $Zn_2(bim)_4$ nanosheets.[28b] After exfoliation of $Zn_2(bim)_3$, the MOF nanosheets were coated on α-Al_2O_3 disks to form ultrathin composite membranes (Figure 6).[28a] The volatile solvent, methanol or propanol, penetrated between the layers of the layered MOFs and stabilized the exfoliated nanosheets. The aperture size of a four-membered ring, ≈ 0.21 nm, helped separate small gas molecules for membrane-based separation applications.

In contrast to exfoliation methods, the surfactant-assisted method is facile for the synthesis of ultrathin layered and nonlayered MOF nanosheets in high yield and can be applied to most MOF structures reported to date.[29] Cao et al. developed a method that used polyvinylpyrrolidone (PVP) as a surfactant molecule that attached onto the MOFs at an early stage in the synthesis and allowed for the vertical growth of MOF crystals, which were referred to as a 2D porphyrin paddlewheel framework-3 (PPF-3).[29a] The thickness of this MOF nanosheet could be tuned by controlling the concentration of the starting materials such that the thickness of the ultrathin PPF-3 nanosheets was 11.9 ± 4.2 nm. These methods developed for 2D MOFs can be applied to modify various structures and properties of MOF nanosheets. Pustovarenko et al. demonstrated the preparation of freestanding lamellae of NH_2-MIL-53(Al), CAU-10(Al), and NH_2-CAU-10(Al).[29c] Surfactant-induced crystal growth of MOFs in the xy-direction resulted in ultrathin nanosheets of MOFs with uniform 3D pore structures (Figure 7). This approach would
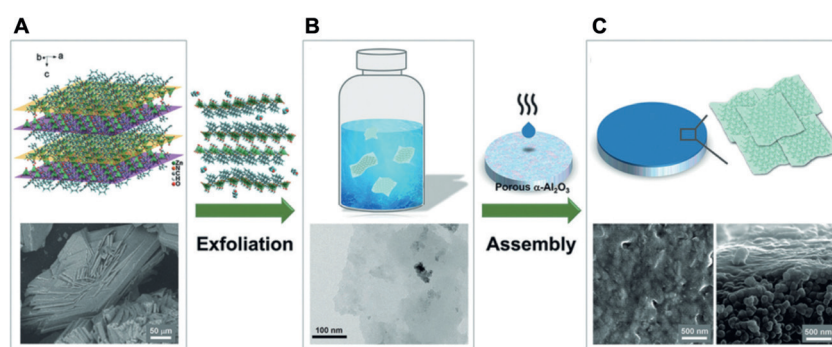
Figure 6. Representation of the precursor exfoliation and nanosheet assembly processes.[28a] A) Top: diagram of a four-layer stack of $Zn_2(Bim)_3$ precursors along the c-axis; bottom: SEM image of the layered precursor particles. The small molecules shown in the exfoliation process represent the methanol and n-propanol. B) Top: $Zn_2(Bim)_3$ nanosheets dispersed in 1:1 v/v methanol/n-propanol; bottom: TEM image of $Zn_2(Bim)_3$ nanosheets. C) Top: illustration of $Zn_2(Bim)_3$ nanosheet membrane; bottom: SEM images of top view (bottom left) and cross-section view (bottom right) of the $Zn_2(Bim)_3$ nanosheet membranes prepared at 200 °C. Copyright 2017, John Wiley and Sons.
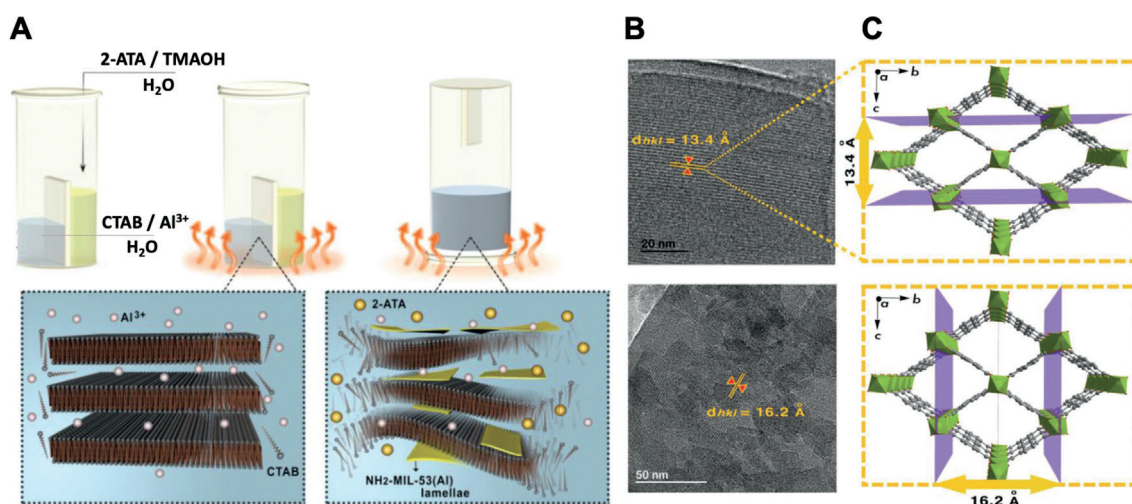
Figure 7. Preparation of 2D MOFs by surfactant-assisted method, A) Schematic representation of the synthetic procedure developed and the formation mechanism of the NH_2-MIL-53(Al) lamellae (synthesis from the aluminum-containing precursor, 2-aminoterephthalic acid (2-ATA), tetramethylammonium hydroxide (TMAOH) as a base to deprotonate, and the cationic surfactant, hexadecyltrimethylammonium bromide (CTAB)). B) HRTEM images acquired for the NH_2-MIL-53(Al) nanosheets. Lattice fringes with interplanar distances of 13.4 and 16.2 Å were observed, corresponding to the crystallographic *c*- and *b*-axis, respectively. C) MIL-53 topology represented along the [100] direction.[29c] Copyright 2018, John Wiley and Sons.

lead to the efficient assembly of any MOFs into ultrathin nanosheets for membrane application.

2.3. Other 2D Materials

Although graphene-based materials and MOFs are of great interest, other 2D materials such as zeolites, molybdenum disulfide, and COFs have shown their potential as 2D materials. Hexagonal layers of boron nitride (BN) and graphitic carbon nitride (g-C_3N_4) are considered as metal-free 2D materials. Transition metal dichalcogenides (TMDs), including MoS_2 and WS_2, in which hexagonal layers of metal atoms (M) are sandwiched between layers of chalcogen atoms (X) in a MX_2 structure, are also promising 2D nanosheet materials. Transition metal carbides or nitrides, known as MXenes with a formula of $M_{n-1}X_nT_x$ (M = transition metal, X = C and/or N, T_x = surface functional group such as F, OH, or O) are also potential membrane materials. Zeolites are synthetic or natural materials with microporous and crystalline properties that are usually used for catalysis, adsorption, and ion exchange applications.[30] Layered intermediates of zeolites, called 2D zeolites, have been developed based on the discovery of a layered precursor available for possible post-synthetic manipulations. Unlike MOFs, COFs are framework materials linked by strong covalent bonds without metal–organic bonds. The functional diversity of the organic linkers expands the possible molecular structures and the range of physical properties.[31] COFs are intrinsically 2D or 3D crystals, depending on their building blocks, and the covalent bond of 2D COFs are restricted to the 2D plane and stacked to form a layered structure. Due to the difficulty in controlling the reaction to crystallize linked organic polymers, methods for reversible formation of covalent bonds are widely used, such as solvothermal synthesis and microwave synthesis.[31]

The synthesized 2D COFs are typically exfoliated nanosheets from layered COFs. Li et al. prepared 2D COF-1 membranes, which were synthesised from 1,4-benzenediboronic acid in a 1,4-dioxane/mesitylene mixture, by ultrafiltration exfoliation followed by assembly on a porous substrate.[32] The 2D COF-1 membranes exhibited decreased surface area, pore volume, and average pore size because of the loss of the original regular channels caused by the random stacking of the nanosheets. However, the nanosheets that were coated in an ultrathin film (thickness of 100 nm) had improved molecular transport properties. Peng et al. prepared COF nanosheets from the synthetic monomer 1,3,5-tris(4-formylphenyl)benzene and the commercial monomers tris(4-aminophenyl)amine and tris(4-formylphenyl)amine; the COF nanosheets had 1.8 nm pores and an interlayer distance of 0.39 nm when stacked (Figure 8).[33] The COFs with highly ordered hexagonal networks and sheet-like morphology were easily exfoliated by ultrasonication due to the weak interlayer stacking force between the flexible building blocks. A facile synthesis of COFs or porous organic frameworks (POFs) is possible when polymer synthesis techniques such as interfacial polymerisation (IP) are applied.[34] Shan et al. developed ultrathin POF membranes, called benzimidazole-linked polymers (BILP-101x), using IP.[34a] The IP method has been applied for the large-scale preparation of polyamide membranes: two different monomers dissolved in different immiscible solvents are reacted at the interface, resulting in ultrathin membranes. A defect-free layer of BILP-101x with a thickness of 400 nm was formed on a porous substrate from an aqueous solution of 1,2,4,5-benzenetetramine tetrahydrochloride (BTA) and a benzene solution of 1,3,5-triformylbenzene (TFB) after a reaction time of few seconds. The use of appropriate monomers enabled the fabrication of microporous and ultrathin membranes. Jimenez-Solomon et al. introduced rigid and contorted structures to synthesize highly
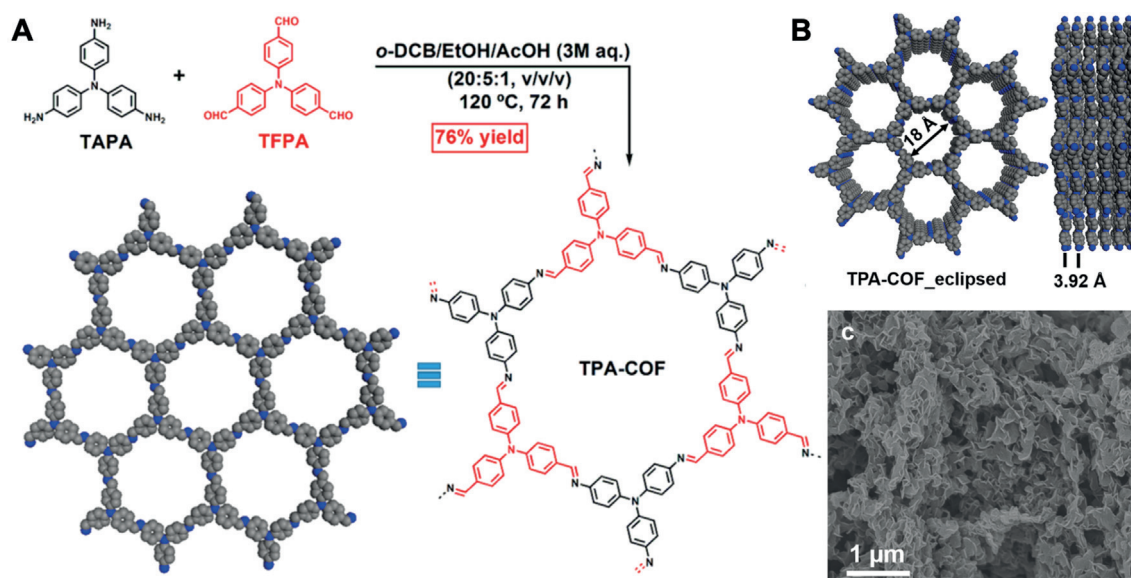
Figure 8. A) Schematic illustration of synthesis and extended hexagonal structure of the bulk TPA-COF material. B) Crystal structure of the bulk TPA-COF material assuming the eclipsed stacking viewed along the [001] (left) and [100] (right) directions with the interlayer distance of 3.92 Å. C) SEM image of the bulk TPA-COF material with sheet-like morphology.[33] Copyright 2017, American Chemical Society.

crosslinked polyarylate nanofilms down to 20 nm in thickness which demonstrated outstanding performance in molecular separation.[34b] Matsumoto et al. reported that imine-linked 2D COFs can be fabricated by the IP method with a use of catalyst.[34c] The membrane thickness was controlled in a range of 2.5 nm to 100 μm such that the amorphous thin film became a crystalline thick film. These methods can be extended to membranes with tunable properties due to the rich chemistry and commercially availability of the monomers, and upscaling is feasible.

Boron nitrides are made up of are hexagonal planes of B and N atoms alternatively linked together via strong B−N covalent bonds. BN is a planar material like graphene, and the crystalline surface of BN brings valuable properties such as high thermal conductivity and mechanical strength. Unlike carbon materials, BN has strong luminescence in the ultraviolet range that makes BN attractive for blue light and ultraviolet emission.[35] BN nanosheets are typically prepared from micrometer-sized, hexagonal BN particles by ultrafiltration with a strong organic solvent.[36] More recently, a low-cost, high-yield preparation method for BN nanosheets by ball milling was developed that was scalable for mass production.[35] During exfoliation, BN nanosheets were functionalized with amino and hydroxyl groups, which increased BN's affinity to other organic molecules. The prepared BN nanosheets consisted of a few layers with a total thickness of 2.5 nm and dimensions below 100 nm (Figure 9a). Functionalized BN nanosheets were introduced into the polymer phase as a filler to improve molecular permeation and separation properties of the polymer membranes without loss of mechanical flexibility (Figure 9b).[35b] Chen et al. also prepared highly water-soluble, functionalized BN by ball milling with urea as a functional agent, and their membrane for solvent separation was fabricated on a porous substrate by vacuum-assisted filtration.[37]

Graphitic carbon nitride has been attractive owing to its tunable properties that can be adopted to various applications such as photocatalysis.[7a] g-C_3N_4 is typically synthesized by thermal polymerization of precursors and their nanosheets are prepared by chemical exfoliation with strong acid, high-temperature calcination under H_2, or sonication-assisted liquid exfoliation depending on the properties of the crude g-C_3N_4.[38] Unlike BN, owing to the small pores of g-C_3N_4 with a geometric diameter of 0.31 to 0.34 nm, 2D membranes of g-C_3N_4 have nanochannels as an extra pathway for the transport of small molecules.[38c]

Transition metal dichalcogenides such as MoS_2, $MoSe_2$, WTe_2, and WS_2 were developed as graphene-like 2D materials with various structures and synthetic routes and widely studied due to their unique electrical, optical, thermal, and mechanical properties.[39] Among them, molybdenum disulfide (MoS_2) and tungsten disulfide (WS_2) are representative 2D materials synthesized by vapor-phase deposition such as sulfurisation, thermal deposition, and vapor-phase reaction.[39a] TMD nanosheets are impermeable materials, but display molecular transport through nanochannels, have antibacterial properties for water filtration, and display high adsorption for certain gases.[40]

$Ti_3C_3T_x$ is one type of widely explored MXene. Owing to its a negatively charged hydrophilic surface, $Ti_3C_3T_x$ displays properties similar to those of GO.[41] Multilayer $Ti_3C_3T_x$ nanosheets are prepared from Ti_3AlC_3 powder by selective etching of the Al layer in acid solution. Then single- or few-layer flakes are prepared by delamination in the aqueous phase by ultrasonication. Representative structures of other 2D materials are described in Figure 10. The preparation of TMDs, g-C_3N_4, and BNs is simpler than that of GO with the possibility of large-scale synthesis.
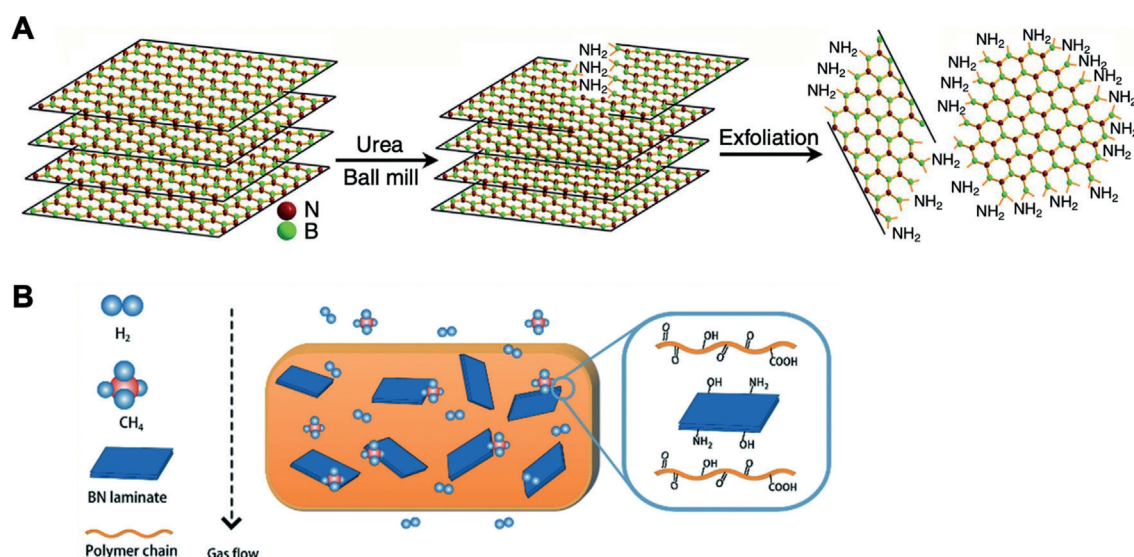
Figure 9. Schematic illustration of the exfoliation and dispersion process. A) Schematic illustration of the exfoliation.[35a] B) Schematic illustration of the structure of functionalized BN–polymer membrane and selective gas permeation through the membrane.[35b] Copyright 2015, Nature Publishing Group. Copyright 2018, John Wiley and Sons.

3. Applications

Nanosheet membranes have demonstrated extraordinary properties in molecular transport but applications are still in the research stage because more investigation for large-scale applications. Membrane processes in ion separation, gas separation, and water processing are well-established industrial processes in which nanosheet membranes will play a great role when large-scale membrane fabrication and modulation methods are achieved. Graphene-based membranes are the pioneers of 2D nanosheet membranes and large-scale membrane fabrication has already have shown potential for ion separation and gas separation. In the first report of GO and rGO membranes by Nair et al. the membranes were impermeable to gas transport of small molecules, but unhindered permeation of water vapor
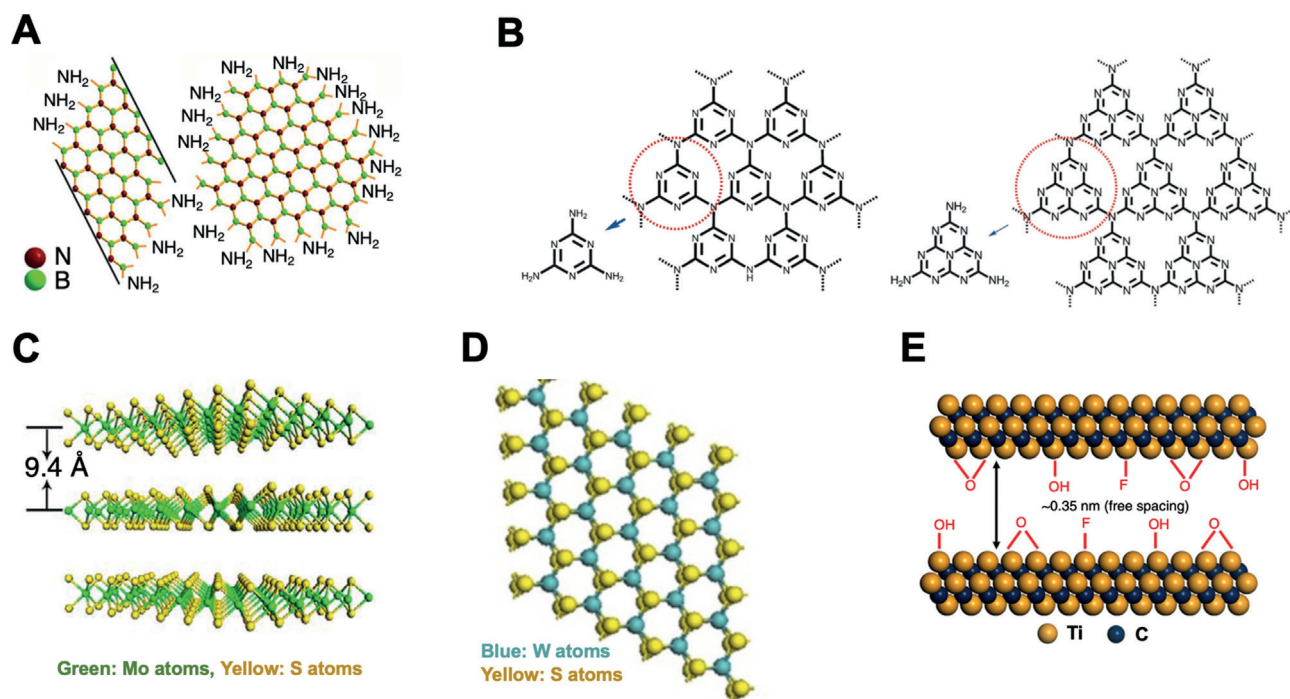
Figure 10. Examples of other 2D materials: A) boron nitride (BN),[35a] B) graphite carbon nitride (g-C₃N₄),[38d] C) molybdenum disulfide (MoS₂),[39e] D) tungsten disulfide (WS₂),[39c] E) MXene.[41c] Copyright 2015, 2018, Nature Publishing Group. Copyright 2012, John Wiley and Sons. Copyright 2013, Springer.

through the membranes showed the possibility of graphene-based materials for membrane separation applications.[42] Ultrathin GO membranes form nanochannels between nanosheets that provide pathways for molecular transport (Figure 11 a).[43] However, their dimensional instability in aqueous
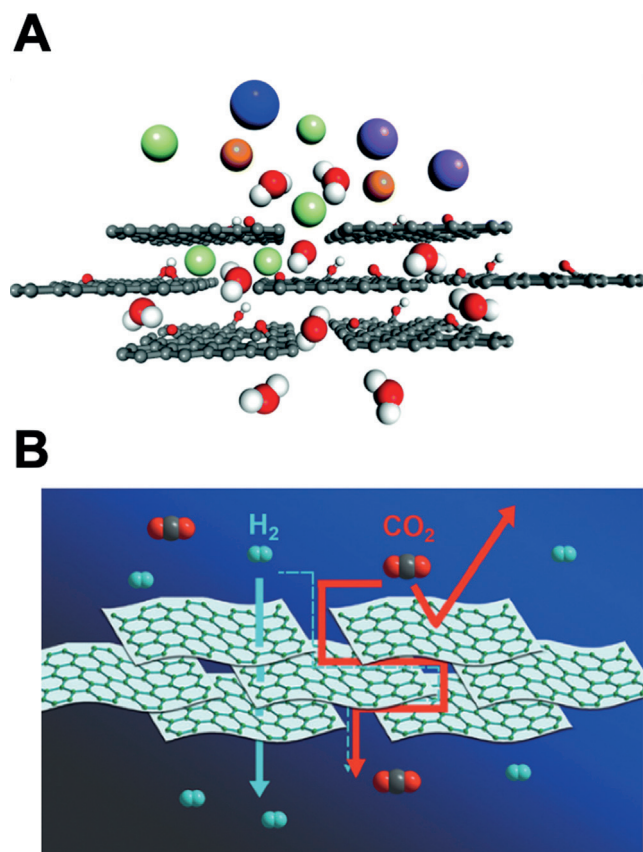
Figure 11. Schematic illustration of molecular transport through 2D nanosheet membranes: A) graphene-based membranes,[43] B) MOF membranes.[28a] Reproduced by permission of The Royal Society of Chemistry, 2016. Copyright 2017, John Wiley and Sons.

or humidified environments limits their practical application. Various methods and materials have been introduced to improve their stability and some of the methods are under investigation for practical applications. Other advanced materials such as MOFs and COFs provide unique molecular transport properties through their highly ordered pores. These membranes have been investigated to minimize membrane thickness with improved physical properties for practical applications, and the methods for nanosheet fabrication have attracted attention to maximize process productivity in membrane processes. Ultrathin MOF or COF membranes form nanochannels between nanosheets as well as nanopores on nanosheets that provide highly selective molecular transport (Figure 11 b);[28a] consequently, membrane processes are highly productive and selective.

3.1. Gas Separation

Molecular transport through nanosheet membranes was first theoretically investigated by quantum mechanical calculations that showed that small pores generated on graphene or GO can enable selective gas transport for certain gases.[44] Stacked graphene and GO also form nanochannels between nanosheets, called the interlayer spacing, and the width of the nanochannels is determined by functional groups of graphene and GO that influence gas permeation and separation properties. Kim et al. demonstrated selective gas transport of small molecules through few-layered GO membranes with a thickness of < 10 nm.[45] The membranes demonstrated ultrafast gas transport of H_2 and selectivity of H_2 over other gases. Interestingly, the gas transport properties varied depending on the experimental conditions such as temperature and humidity. GO membranes are likely to swell in high-humidity environments that increase the interlayer spacing between the GO nanosheets. Water molecules accumulated in the nanochannels hinder gas transport, except for CO_2 transport. Usually the gas transport properties of conventional polymer membranes change with temperature and humidity mainly due to changes in gas activation behavior,[46] but for GO membranes, the gas transport properties change because the nanochannel structure becomes unstable.

One approach to improve the mechanical properties of a membrane and form an ultrathin layer is to crosslink the GO nanosheets with borate. Wang et al. prepared a GO–borate membrane with a thickness of 8 nm by vacuum-assisted filtration and thermal treatment.[47] Depending on the thermal treatment temperature, the interlayer spacing was controlled between 0.68 and 0.79 nm. The change in the interlayer spacing between wet and dry states was small, and the membrane did not lose separation performance in a humidified state with an industrial gas stream. The membrane had a CO_2 permeance of 650 GPU (1 GPU $= 10^{-6}$ cm^3(STP) cm^{-2} s^{-1} cmHg$^{-1} = 3.3 \times 10^{-10}$ mol m^{-2} s^{-1} Pa^{-1}) and selectivity of 75 over methane (CO_2/CH_4), which exceeded that of other GO membranes and was even comparable to that of zeolites or ultrathin polymers. Yan et al. introduced a small amount of GO to a chitosan membrane and followed the crosslinking with borate with a thermal treatment to improve its mechanical and barrier properties. They found that only 1.0 wt % each of boron and GO in chitosan increased the tensile strength by 160 % and the original oxygen permeability was surpassed by 10 %.[48] This was mainly because the GO nanosheets and crosslinked network increased the tortuosity of the pathway for gas transport and decreased the gas diffusion. Yang et al. prepared thiourea-crosslinked GO (TU-GO) membranes through a facile hydrothermal self-assembly synthesis by immersing a ceramic support tube in a GO and thiourea solution at 80 °C under alkaline conditions (pH 8) which caused covalent crosslinking.[49] The thickness of the TU-GO layer was controlled from 70 nm to several microns by using a controlled reaction time and solution concentration. The membrane presented a unique H_2 permeance of over 68×10^{-8} mol m^{-2} s^{-1} Pa^{-1} (2060 GPU) and an ideal selectivity of

over 150 for H_2 over any other gas molecules. The membrane also underwent dehydration via a pervaporation process that demonstrated nearly complete rejection of alcohol and ions while water vapor was permeated.

GO nanosheets serve as building blocks or scaffolds for ultrathin membranes, although they are often used to suppress gas transport and improve barrier properties. Because membrane thickness is important to increase gas permeance, membrane fabrication with an ultrathin membrane layer has been investigated. Unfortunately, defects in the membrane often eliminated its separation properties. Kim et al. introduced GO nanosheets into polybenzoxazole-co-imide, called a thermally rearranged polymer, with a thickness of 35 nm.[50] A polymer solution with GO nanosheets was spin-coated on an AAO disc as a substrate and GO nanosheets uniformly coated the substrate without defects. The membrane demonstrated an improved CO_2 permeance of 1784 GPU while maintaining a gas selectivity that was 482 times higher than that of the freestanding membrane film.

MOFs have been widely investigated as gas separation membranes due to their unique crystalline and pore structures. 2D MOFs provide well-ordered nanopores as well as nanochannels that are advantageous for membrane applications. MOF membranes are typically introduced as a thin-film composite on a substrate or a MOF–polymer composite, called a mixed-matrix membrane (MMM), but micron-sized 3D crystals often agglomerate and restrict the integration of MOFs in the polymer phase. 2D nanosheet fillers of MOFs are advantageous in incorporating them into polymers or building ultrathin 2D membranes for membrane processes. Rodenas et al. focused on copper 1,4-benzenedicarboxylate (CuBDC) MOF; they synthesized MOF nanosheets by the diffusion-mediated modulation of the MOF growth kinetics.[51] The MOF crystal morphology evolved based on the synthesis temperature, from ultrathin nanosheets (< 10 nm) at 298 K to thicker platelets at 333 K. The same methodology can be adapted to other layered MOFs by using alternative metal nodes such as Co^{2+} and Zn^{2+} to tune the porosity and functionality of MOFs. These 2D MOF nanosheets were incorporated into a commercial PI called Matrimid® 5218 to fabricate MMMs and MOF nanosheets that were uniformly distributed through the entire membrane, whereas the regular MOF crystals usually displayed fractures or defects between crystals and the polymer phases. Pustovarenko et al. prepared nonlayered MOF nanosheets through a surfactant-assisted method and fabricated MMMs with Matrimid® 5218.[29c] This membrane presented an improvement of CO_2 permeability over that of pristine Matrimid® 5218 by almost 200% as well as CO_2/CH_4 selectivity after addition of 16 wt% MOF nanosheets. Peng et al. prepared poly(Zn_2(benzimidazole)$_4$) (Zn_2(bim)$_4$) nanosheet membranes coated on α-Al_2O_3 discs as molecular sieve nanosheets.[28b] Zn_2(bim)$_4$ nanosheets were prepared from bulk Zn_2(bim)$_4$ by ball milling and were coated by vacuum filtration. The resulting membrane demonstrated H_2 permeance of up to 2700 GPU with H_2/CO_2 selectivity of 291. Wang et al. introduced the Ni_8(5-bbdc)$_6$(μ-OH)$_4$) structure, called the Mesh Adjustable Molecular Sieve (MAMS-1) due to its excellent hydrothermal stability and 2D layered structure with interplanar distances of 2.9 and 5.0 Å.[52]

MAMS-1 membranes presented a sharp cutoff of the permeance between He and H_2 gases and larger molecular gases. Hu et al. incorporated GO as a seeding layer during ZIF-8 synthesis and formed ZIF-8/GO nanosheet membranes on AAO as well as on nylon substrates.[53] Incorporating GO into ZIF-8 greatly reduced the membrane thickness to ≈ 100 nm and improved gas permeance. The membrane had an H_2 permeance of over 5.46×10^{-8} mol m^{-2} s^{-1} Pa^{-1} (165 GPU). Similarly, g-C_3N_4 was also used as a template layer for ZIF-8, and the resulting membrane exhibited H_2 permeance of 203 GPU.[54] Shan et al. prepared an ultrathin layer of BILP-101x on a γ-Al_2O_3 support by IP that along with high temperature stability exhibited H_2 permeance of up to 24.3 GPU with H_2/CO_2 selectivity of 39.7.[34a]

Other 2D materials, such as COFs, MXenes, MoS_2, WS_2, BN, and g-C_3N_4 were also tested in gas separation applications. Ultrathin MoS_2 membranes prepared by Wang et al. showed very high H_2 permeance up to 27 440 GPU based on Knudsen diffusion.[55] Freestanding 2D MXene membranes with a thickness of 2 μm prepared by Ding et al. presented excellent H_2 permeability and selectivity over other gases (H_2/ CO_2 selectivity of 160) with stable long-term performance over 700 h of continuous operation.[41c] Another MXene membrane fabricated by Shen et al. on an AAO substrate by vacuum filtration presented a defect-free layer with a controllable thickness of 5 to 80 nm.[56] This MXene membrane demonstrated precise H_2 transport with H_2 permeance of 1584 GPU and H_2/CO_2 selectivity of 27. However, after crosslinking with borate and polyethylenimine and following 75 °C treatment (MBP-75), the CO_2 permeance was remarkably enhanced. Nanosheets such as WS_2 or BN can be incorporated into polymer phase to form mixed-matrix membranes with gas permeability and/or selectivity. The introduction of 10% WS_2 into fluorinated poly(phenylene oxide) (FPPO) improved CO_2 permeability, CO_2/N_2 selectivity, and CO_2/CH_4 selectivity by 216%, 148%, and 137%, respectively, because WS_2 provided transport channels for gas molecules.[40c] Similarly, introduction of functionalized BN nanosheets (1 wt%) into thermally rearranged polymers increased H_2/CH_4 selectivity from 24.1 to 275.[35b]

Table 1 summarizes the gas transport properties of 2D nanocomposite membranes based on GO and MOFs. Not many membranes with remarkable performance have been reported, but the number of investigated 2D nanocomposite membranes is growing. When nanosheets were introduced as scaffolds for membrane fabrication, their gas transport properties were mostly affected by the properties of the precursors. In this case, gas selectivity was maintained, but gas permeance was significantly increased because of the reduced membrane thickness of the nanosheets. MOF-based 2D membranes exhibited greater H_2 permeance, which came from the intrinsic properties of MOFs because MOF membranes usually provide unique nanopores suitable for H_2 molecular transport.

Table 1: Gas permeation and separation properties of 2D nanocomposite membranes.

Sample	Gas permeance (GPU)[a]				Ideal gas selectivity		
	H_2	CO_2	N_2	CH_4	α_{H_2/CO_2}	α_{CO_2/N_2}	α_{CO_2/CH_4}
GO (dry)[45]	35	1.17	10	15	30	0.12	0.08
GO (hydrated)[45]	8.5	45	2.5	2	0.19	18	22.5
B-GO/PES[47]		650	11.4	8.67		57	75
TU-GOF-1[49]	2642	311	867	203	8.5	0.36	1.5
TU-GOF-3[49]	637	6.36	13.0	5.45	100	0.49	1.2
TU-GOF-5[49]	327	10.3	16.7	17.6	32	0.62	0.59
TU-GOF/Ceramic[49]	2060	9.16	11.2	7.25	225	0.82	1.3
rGO-PBOI-1.0[50]	1847	1784	101	55.1	1.0	18	32
rGO-PBOI-1.5[50]	1505	1450	76.0	41.7	1.0	19	35
rGO-PBOI-2.0[50]	1233	1149	56.4	29.4	1.1	20	39
rGO-PBOI-2.2[50]	986	872	41.7	20.3	1.1	21	43
rGO-PBOI-2.4[50]	761	673	30.7	15.1	1.1	22	45
$Zn_2(bim)_4$ M2[28b]	3730	15.7			238		
$Zn_2(bim)_4$ M3[28b]	3760	22.8			165		
$Zn_2(bim)_4$ M7[28b]	2670	9.7			275		
$Zn_2(bim)_4$ M8[28b]	2270	10.5			216		
$Zn_2(bim)_4$ M9[28b]	2700	9.3			290		
ZIF-8/GO[53]	165	104	14.9	14.7	1.6	7.0	7.1
ZIF-8/g-C_3N_4[54]	203	4.85		5.64	42		0.86
BILP-101x(3)[56]	24.3	0.61			39.7		
BILP-101x(4)[56]	14.7	0.68			21.6		
MoS_2 17 nm[55]	27440	8135	9196	11495	3.4	0.88	0.71
MoS_2 35 nm[55]	7044	1916	2299	3065	3.7	0.83	0.63
MoS_2 60 nm[55]	2446	560	780	884	4.4	0.72	0.63
MAMS-1 12 nm[52]	7640	255			30		
MAMS-1 40 nm[52]	715	2.67	5.81	4.36	268	0.46	0.61
MXene 20 nm[56]	1584	58.7			27		
MBP-75 20 nm[56]		350		22.9			15.3

[a] 1 GPU $= 10^{-6}$ cm^3(STP) cm^{-2} s^{-1} cmHg$^{-1} = 3.3 \times 10^{-10}$ mol m^{-2} s^{-1} Pa^{-1}.

3.2. Ion Separation

Ion separation is a widely applied process in water treatment and in the food, chemical, and pharmaceutical industries.[1] Nanosheet membranes were first used in ion separation applications for water or liquid treatment processes such as nanofiltration and ultrafiltration.[57] Although Joshi et al. reported that the GO laminates presented a sharp molecular cutoff at 0.45 nm for ion and molecular sieving,[58] their natural tendency to swell in the aqueous state increased their instability in water.[14] Preventing their swelling during the separation process and maintaining high membrane performance are the key issues for graphene-based membranes.

Crosslinking graphene or GO nanosheets is the most commonly considered method to prevent the swelling of nanosheets because the chemical bonds created at the crosslinking sites limit the dispersion of the nanosheets in water. Jia et al. introduced the covalent crosslinking of GO membranes with dicarboxylic acid.[13] After the formation of a GO layer on a substrate, dicarboxylic acid crosslinking agents with different chain lengths and structures were introduced that varied the interlayer distance of the GO nanosheets. Depending on the crosslinking agents used, the mechanical properties and permeation flux of the membrane for various ions changed. For a pristine GO membrane, the ion permeation flux of KCl and $K_4[Fe(CN)_6]$ were similar, but after crosslinking, the KCl flux showed a minor increase, but the $K_4[Fe(CN)_6]$ flux decreased. In contrast, when GO nanosheets were crosslinked with a long linear crosslinker, octanedioic acid, the membrane demonstrated a major flux increase for both KCl and $K_4[Fe(CN)_6]$. Controlled crosslinking by the use of the salt mixture KCl + M (M = NaCl, CaCl$_2$, LiCl, or MgCl$_2$) led to a GO membrane with ion sieving.[19b] A KCl-treated GO membrane with a thickness of 750 nm showed low permeation rates for Na$^+$, Mg^{2+}, and Ca^{2+} below the detection rate in the single-ion permeate test. The ion flux changes were mainly due to the size-selectivity of hydrate ions from the different interlayer spacings. Lim et al. introduced GO membranes crosslinked to polyethyleneimine (PEI) with tannic acid (TA) under alkaline conditions (pH 8.5) in which TA reacts well with GO by oxidative coupling polymerization and with the amine groups on PEI, improving the dimensional stability.[59] The crosslinked membrane exhibited a high water flux of 15.4 L m^{-2} h^{-1} with NaCl and MgSO$_4$ rejection of 66 % and 82 %, respectively. This GO-based membrane also showed great antibacterial properties, mainly due to the TA moiety.

Abraham et al. reported a GO membrane that exhibited tunable sieving of ions.[60] Physically confined GO nanosheets in a sealed container were naturally swelled under different humidity conditions to control their interlayer spacing and were immediately glued. The interlayer spacing of GO nanosheets increased linearly with the relative humidity during preparation. The ion permeation rates exponentially decreased with decreasing channel size, but the effects on water transport were weak. The graphene-based membranes exhibited 97 % rejection for NaCl; this indicated a possible route for desalination applications. Akbari et al. prepared GO large-area nanofiltration membranes by casting concentrated GO ink; the membranes exhibited retention of salts (MgCl$_2$, Na$_2$SO$_4$, NaCl, and MgSO$_4$) around 30 to 37 %. In this case, modification might improve the salt rejection properties.[20]

MOF membranes with a narrow pore size distribution are also of great interest for ion separation applications. Well-defined pore structures can lead to selective ion transport. Zhang et al. prepared an ultrathin ZIF-8 membrane by GO-assisted interfacial growth on AAO substrate; the membrane quickly and selectively transports Li$^+$ over other alkali metal ions.[61] A ZIF-8/GO layer was formed with a thickness of $\approx$ 400 nm and $\approx$ 200-nm-sized ZIF-8 crystals were observed.

Ion transport properties were mainly based on the pore size of the MOFs and the ion diameters. The ion selectivity of the ZIF-8/GO membranes for Li^+/Rb^+, Li^+/K^+, and Li^+/Na^+ were 4.6, 2.2, and 1.4, respectively, which was the highest ever reported for synthetic membranes due to the small difference in ionic diameters.

Unlike GO membranes, MoS_2 membranes demonstrated excellent antiswelling with a stable interlayer spacing of 1.2 nm without nanosheet crosslinking, which was advantageous for the synthesis.[39b] The 500 nm thick MoS_2 membrane presented a high water flux of 140 $L\,m^{-2}\,h^{-1}$ at 0.7 bar, but ion separation performance was around 55 to 70%. A g-C_3N_4 membrane 160 nm thick coated on a AAO support also demonstrated high water flux in the nanofiltration range but showed no ion rejection performance.[38e]

3.3. Water Desalination

Membrane-based water desalination is one of the most widely applied processes to produce potable water from saline water. Hydraulic pressure is typically applied for a reverse osmosis (RO) process and osmotic pressure applied for a forward osmosis (FO) process. However, not many materials are suitable for this process due to limitations in performance, and some polymer membranes such as CA and PA in thin-film composites dominate the membrane desalination market.[62] Despite the great molecular transport of water molecules through GO membranes, because of dimensional stability they have a low rejection of small ions such as NaCl, which is a major component to be removed from salt water.[14] Numerous graphene-based membranes have been investigated to improve salt rejection properties for water desalination processes, but not many membranes exhibited sufficiently high salt rejection to be suitable for practical desalination applications.

FO processes do not require excessive mechanical properties because high pressure is not applied on the membranes to drive water transport. Therefore, ultrathin freestanding membranes can be used for the FO process. Liu et al. prepared freestanding, ultrathin reduced GO membranes that exhibited high water flux and salt rejection in an FO process with minimized internal concentration polarization issues.[63] The GO solution was first applied to a cellulose nitrate membrane filter by the vacuum filtration method, then delaminated under hydriodic acid vapor. The GO was reduced during delamination by exposure to acid vapor and a freestanding GO membrane was obtained. The membrane thickness was controlled from 20 nm to 500 nm and the membrane with 100 nm thickness demonstrated a water flux of around 25 $L\,m^{-2}\,h^{-1}$. Moreover, rGO membranes presented much lower ion permeability than GO membranes or commercial cellulose triacetate membranes. Chemical crosslinking of GO with PA is the way to develop desalination membranes because PA is widely used for membrane desalination processes. Jin et al. introduced crosslinking of GO with diamine and trimethyl chloride monomers by using amide-bonding between the acid groups on the GO and the amide groups of the crosslinker, and inter-crosslinking

between parallel GO nanosheets was achieved by formation of a PA structure.[64]

Physical crosslinking of GO nanosheets by entwining them with a network polymer is one way to prevent the swelling of GO membranes. Kim et al. introduced the network polymer poly(NIPAM-MBA) into a GO nanosheet during membrane preparation for use in RO and FO applications. This crosslinking method suppressed the swelling of GO nanosheets in water and improved their salt rejection capability while maintaining their water flux. The membrane prepared on a nylon substrate by spin-coating, with a thickness of less than 40 nm, demonstrated a water flux of 25.8 $L\,m^{-2}\,h^{-1}$ and NaCl rejection of 99.9% in the FO process.[22c] The membrane fabricated by casting and filtration method exhibited a water flux of 33.5 $L\,m^{-2}\,h^{-1}$ with NaCl rejection of 98.5% at 10 bar in an RO process.[23] This membrane also showed great chlorine tolerance that significantly simplified the desalination process and extended membrane lifetime because oxidation agents, such as chlorine, that are widely used for disinfection during water processing, are likely to degrade membrane structures. The preparation method based on casting and vacuum filtration showed potential for large-scale membrane fabrication because continuous casting is the way to produce flat sheet membranes at an industrial scale. Crosslinking of GO/FLG layers by thermal treatment and Ca^{2+} crosslinking with DOC greatly improved the NaCl rejection of the membrane to 85% and mechanical resistance to 50 bar.[21] The NaCl rejection mechanism is due to Gibbs–Donnan exclusion by the surface functional groups of GO and DOC, and the zwitterionic behavior by the combination of Ca^{2+} and DOC.

4. Summary and Outlook

The recent development of 2D materials and their composite membranes have opened the next generation in membrane processes for gas, ion, and liquid separations. Following the development of chemical or physical exfoliation, as well as in situ fabrication methods to prepare 2D materials, their membrane applications have been investigated, resulting in the formation of ultrathin layers with well-ordered nanopores and/or nanochannels. The pioneering GO-based membranes presented remarkable performance in gas separation and possible liquid separation. Crosslinking of GO membranes by chemical or physical methods improved dimensional stability of GO membranes in water, qualifying them for water desalination applications with long-term performance stability. Developments in the fabrication of graphene-based membranes from modified GO solution demonstrated potential for large-scale manufacturing by conventional methods such as casting, spin-coating, and spray-coating that have been applied for polymer-based membranes. Crosslinking of GO also makes it possible to tune the size of nanochannels that effect molecular transport, improving the rejection of monovalent and divalent ions. Other 2D materials such as MOFs, COFs, BNs, g-C_3N_4, TMDs, and MXene were fabricated into ultrathin composite membranes by solution filtration or interfacial polymeri-

zation, or into mixed matrix membranes with organic polymers. They demonstrated great molecular transport properties. Their intrinsic stability based on their firm crystalline structure has improved the stability of the membranes. Functionalization of the 2D materials also improved their affinity with polymers when they were mixed to form polymer nanocomposites. The inherent nanosized pores of MOFs and COFs are also advantageous for molecular transport. It is anticipated that the development of 2D MOFs or COFs will bring a breakthrough for membrane applications.

Despite the great progress achieved, several emerging challenges remain for industrial applications of 2D-based membranes. First, scalable preparation methods for 2D materials with controlled properties should be developed. The latest 2D materials, such as 2D MOFs and BN, require complex synthetic methodology or lengthy reaction time from low concentration solution which leads to much effort in preparation and produces vast volume of liquid waste. Some 2D materials such as COFs also require synthetic monomers. Although graphene-based materials are prepared in aqueous solution on a large scale, the quality of the precursors from the manufacturing sources should be controlled. Second, the properties of dispersed GO in water led to performance instability of those membranes and poor salt rejection properties in water processing. The intrinsic degradation of MOFs in water also hinders their application in water desalination, therefore a breakthrough in materials development is essential, considering the market size of membrane liquid separations. Lastly, issues concerning membrane fabrication in uniform quality remain. Controlled solution-based methods can be used to prepare ultrathin membrane layers of 2D materials by filtration coating that are not feasible for continuous membrane fabrication process. Although a study showed GO membrane fabrication by casting of GO ink, modification is required for higher separation performance. To be successfully applied for industrial membrane processes, membrane fabrication over large areas and modulation are essential to deal with the large volume of raw substances to be purified in a continuous process. Membrane fabrication in thin-film composites or hollow fibers, the industrial standard for membrane formation, would make 2D nanosheet membranes an attractive alternative to current polymer-based membranes, but it requires other strategies for materials research investigations. Proper incorporation of 2D materials in polymers as templates to improve the original performance of polymer membranes will also be a promising and relatively facile method to advance their performance. Various approaches to overcome the current challenges in 2D membranes will advance membrane processes and lead to further potential uses in nanofiltration and energy-related applications.

Acknowledgements

Conflict of interest

The authors declare no conflict of interest.

How to cite: *Angew. Chem. Int. Ed.* **2019**, *58*, –
Angew. Chem. **2019**, *131*, –

[1] J. Mulder, *Basic principles of membrane technology*, Springer Science & Business Media, Berlin, **1996**.

[2] Y. Cohen, R. Semiat, A. Rahardianto, *AIChE J.* **2017**, *63*, 1771–1784.

[3] S. Kim, Y. M. Lee, *Prog. Polym. Sci.* **2015**, *43*, 1–32.

[4] S. S.-Y. Chui, S. M.-F. Lo, J. P. H. Charmant, A. G. Orpen, I. D. Williams, *Science* **1999**, *283*, 1148–1150.

[5] X.-H. Liu, C.-Z. Guan, S.-Y. Ding, W. Wang, H.-J. Yan, D. Wang, L.-J. Wan, *J. Am. Chem. Soc.* **2013**, *135*, 10470–10474.

[6] K. Toda, R. Furue, S. Hayami, *Anal. Chim. Acta* **2015**, *878*, 43–53.

[7] a) M. Xu, T. Liang, M. Shi, H. Chen, *Chem. Rev.* **2013**, *113*, 3766–3798; b) M. Naguib, V. N. Mochalin, M. W. Barsoum, Y. Gogotsi, *Adv. Mater.* **2014**, *26*, 992–1005; c) G. R. Bhimanapati, Z. Lin, V. Meunier, Y. Jung, J. Cha, S. Das, D. Xiao, Y. Son, M. S. Strano, V. R. Cooper, *ACS Nano* **2015**, *9*, 11509–11539; d) H. Huang, Y. Ying, X. Peng, *J. Mater. Chem. A* **2014**, *2*, 13772–13782; e) G. Liu, W. Jin, N. Xu, *Chem. Soc. Rev.* **2015**, *44*, 5016–5030; f) G. Liu, W. Jin, N. Xu, *Angew. Chem. Int. Ed.* **2016**, *55*, 13384–13397; *Angew. Chem.* **2016**, *128*, 13580–13595; g) X. Q. Cheng, Z. X. Wang, X. Jiang, T. Li, C. H. Lau, Z. Guo, J. Ma, L. Shao, *Prog. Mater. Sci.* **2018**, *92*, 258–283.

[8] D. Chen, H. Feng, J. Li, *Chem. Rev.* **2012**, *112*, 6027–6053.

[9] Y. Q. Li, T. Yu, T. Y. Yang, L. X. Zheng, K. Liao, *Adv. Mater.* **2012**, *24*, 3426–3431.

[10] K. W. Putz, O. C. Compton, M. J. Palmeri, S. T. Nguyen, L. C. Brinson, *Adv. Funct. Mater.* **2010**, *20*, 3322–3329.

[11] Z. An, O. C. Compton, K. W. Putz, L. C. Brinson, S. T. Nguyen, *Adv. Mater.* **2011**, *23*, 3842–3846.

[12] W. Cui, M. Li, J. Liu, B. Wang, C. Zhang, L. Jiang, Q. Cheng, *ACS Nano* **2014**, *8*, 9511–9517.

[13] Z. Jia, Y. Wang, *J. Mater. Chem. A* **2015**, *3*, 4405–4412.

[14] S. Zheng, Q. Tu, J. J. Urban, S. Li, B. Mi, *ACS Nano* **2017**, *11*, 6440–6450.

[15] a) Y. T. Nam, J. Choi, K. M. Kang, D. W. Kim, H.-T. Jung, *ACS Appl. Mater. Interfaces* **2016**, *8*, 27376–27382; b) W.-S. Hung, C.-H. Tsou, M. De Guzman, Q.-F. An, Y.-L. Liu, Y.-M. Zhang, C.-C. Hu, K.-R. Lee, J.-Y. Lai, *Chem. Mater.* **2014**, *26*, 2983–2990.

[16] J. W. Burress, S. Gadipelli, J. Ford, J. M. Simmons, W. Zhou, T. Yildirim, *Angew. Chem. Int. Ed.* **2010**, *49*, 8902–8904; *Angew. Chem.* **2010**, *122*, 9086–9088.

[17] P. Song, Z. Xu, Y. Wu, Q. Cheng, Q. Guo, H. Wang, *Carbon* **2017**, *111*, 807–812.

[18] Y. Zhang, S. Japip, T.-S. Chung, *Carbon* **2017**, *123*, 193–204.

[19] a) S. Park, K.-S. Lee, G. Bozoklu, W. Cai, S. T. Nguyen, R. S. Ruoff, *ACS Nano* **2008**, *2*, 572–578; b) L. Chen, G. Shi, J. Shen, B. Peng, B. Zhang, Y. Wang, F. Bian, J. Wang, D. Li, Z. Qian, *Nature* **2017**, *550*, 380; c) C.-N. Yeh, K. Raidongia, J. Shao, Q.-H. Yang, J. Huang, *Nat. Chem.* **2015**, *7*, 166.

[20] A. Akbari, P. Sheath, S. T. Martin, D. B. Shinde, M. Shaibani, P. C. Banerjee, R. Tkacz, D. Bhattacharyya, M. Majumder, *Nat. Commun.* **2016**, *7*, 10891.

[21] A. Morelos-Gomez, R. Cruz-Silva, H. Muramatsu, J. Ortiz-Medina, T. Araki, T. Fukuyo, S. Tejima, K. Takeuchi, T. Hayashi, M. Terrones, *Nat. Nanotechnol.* **2017**, *12*, 1083.

[22] a) H. Bai, C. Li, X. Wang, G. Shi, *Chem. Commun.* **2010**, *46*, 2376–2378; b) M. Zhong, Y.-T. Liu, X.-M. Xie, *J. Mater. Chem. B* **2015**, *3*, 4001–4008; c) S. Kim, X. Lin, R. Ou, H. Liu, X. Zhang, G. P. Simon, C. D. Easton, H. Wang, *J. Mater. Chem. A* **2017**, *5*, 1533–1540.

[23] S. Kim, R. Ou, Y. Hu, X. Li, H. Zhang, G. P. Simon, H. Wang, *J. Membr. Sci.* **2018**, *562*, 47–55.

[24] a) H. Furukawa, K. E. Cordova, M. O'Keeffe, O. M. Yaghi, *Science* **2013**, *341*, 1230444; b) M. Zhao, Y. Huang, Y. Peng, Z. Huang, Q. Ma, H. Zhang, *Chem. Soc. Rev.* **2018**, *47*, 6267–6295.

[25] S. L. James, *Chem. Soc. Rev.* **2003**, *32*, 276–288.

[26] J. Yao, H. Wang, *Chem. Soc. Rev.* **2014**, *43*, 4470–4493.

[27] M. Zhao, Q. Lu, Q. Ma, H. Zhang, *Small Methods* **2017**, *1*, 1600030.

[28] a) Y. Peng, Y. Li, Y. Ban, W. Yang, *Angew. Chem. Int. Ed.* **2017**, *56*, 9757–9761; *Angew. Chem.* **2017**, *129*, 9889–9893; b) Y. Peng, Y. Li, Y. Ban, H. Jin, W. Jiao, X. Liu, W. Yang, *Science* **2014**, *346*, 1356–1359.

[29] a) F. Cao, M. Zhao, Y. Yu, B. Chen, Y. Huang, J. Yang, X. Cao, Q. Lu, X. Zhang, Z. Zhang, C. Tan, H. Zhang, *J. Am. Chem. Soc.* **2016**, *138*, 6924–6927; b) Y. Wang, M. Zhao, J. Ping, B. Chen, X. Cao, Y. Huang, C. Tan, Q. Ma, S. Wu, Y. Yu, *Adv. Mater.* **2016**, *28*, 4149–4155; c) A. Pustovarenko, M. G. Goesten, S. Sachdeva, M. Shan, Z. Amghouz, Y. Belmabkhout, A. Dikhtiarenko, T. Rodenas, D. Keskin, I. K. Voets, *Adv. Mater.* **2018**, *30*, 1707234.

[30] W. J. Roth, P. Nachtigall, R. E. Morris, J. Čejka, *Chem. Rev.* **2014**, *114*, 4807–4837.

[31] X. Feng, X. Ding, D. Jiang, *Chem. Soc. Rev.* **2012**, *41*, 6010–6022.

[32] G. Li, K. Zhang, T. Tsuru, *ACS Appl. Mater. Interfaces* **2017**, *9*, 8433–8436.

[33] Y. Peng, Y. Huang, Y. Zhu, B. Chen, L. Wang, Z. Lai, Z. Zhang, M. Zhao, C. Tan, N. Yang, F. Shao, Y. Han, H. Zhang, *J. Am. Chem. Soc.* **2017**, *139*, 8698–8704.

[34] a) M. Shan, X. Liu, X. Wang, I. Yarulina, B. Seoane, F. Kapteijn, J. Gascon, *Sci. Adv.* **2018**, *4*, eaau1698; b) M. F. Jimenez-Solomon, Q. Song, K. E. Jelfs, M. Munoz-Ibanez, A. G. Livingston, *Nat. Mater.* **2016**, *15*, 760; c) M. Matsumoto, L. Valentino, G. M. Stiehl, H. B. Balch, A. R. Corcos, F. Wang, D. C. Ralph, B. J. Mariñas, W. R. Dichtel, *Chem* **2018**, *4*, 308–317.

[35] a) W. Lei, V. N. Mochalin, D. Liu, S. Qin, Y. Gogotsi, Y. Chen, *Nat. Commun.* **2015**, *6*, 8849; b) Y. Wang, Z. X. Low, S. Kim, H. Zhang, X. Chen, J. Hou, J. G. Seong, Y. M. Lee, G. P. Simon, C. H. Davies, *Angew. Chem. Int. Ed.* **2018**, *57*,, 16056—16061; *Angew. Chem.* **2018**, *130*, 16288–16293.

[36] C. Zhi, Y. Bando, C. Tang, H. Kuwahara, D. Golberg, *Adv. Mater.* **2009**, *21*, 2889–2893.

[37] C. Chen, J. Wang, D. Liu, C. Yang, Y. Liu, R. S. Ruoff, W. Lei, *Nat. Commun.* **2018**, *9*, 1902.

[38] a) J. Xu, L. Zhang, R. Shi, Y. Zhu, *J. Mater. Chem. A* **2013**, *1*, 14766–14772; b) J. Liu, H. Wang, M. Antonietti, *Chem. Soc. Rev.* **2016**, *45*, 2308–2326; c) Z. Tian, S. Wang, Y. Wang, X. Ma, K. Cao, D. Peng, X. Wu, H. Wu, Z. Jiang, *J. Membr. Sci.* **2016**, *514*, 15–24; d) Y. Wang, X. Wang, M. Antonietti, *Angew. Chem. Int. Ed.* **2012**, *51*, 68–89; *Angew. Chem.* **2012**, *124*, 70–92; e) Y. Wang, L. Li, Y. Wei, J. Xue, H. Chen, L. Ding, J. Caro, H. Wang, *Angew. Chem. Int. Ed.* **2017**, *56*, 8974–8980; *Angew. Chem.* **2017**, *129*, 9102–9108.

[39] a) Y. Shi, H. Li, L.-J. Li, *Chem. Soc. Rev.* **2015**, *44*, 2744–2756; b) Z. Wang, Q. Tu, S. Zheng, J. J. Urban, S. Li, B. Mi, *Nano Lett.* **2017**, *17*, 7289–7298; c) X. Mao, Y. Xu, Q. Xue, W. Wang, D. Gao, *Nanoscale Res. Lett.* **2013**, *8*, 430; d) M. Chhowalla, H. S. Shin, G. Eda, L.-J. Li, K. P. Loh, H. Zhang, *Nat. Chem.* **2013**, *5*, 263; e) M.-R. Gao, M. K. Chan, Y. Sun, *Nat. Commun.* **2015**, *6*, 7493.

[40] a) L. Sun, Y. Ying, H. Huang, Z. Song, Y. Mao, Z. Xu, X. Peng, *ACS Nano* **2014**, *8*, 6304–6311; b) Z. Geng, Q. Song, X. Zhang, B. Yu, Y. Shen, H. Cong, *J. Membr. Sci.* **2018**, *565*, 226–232; c) P. Cheng, Y. Chen, X. Yan, Y. Wang, W. Z. Lang, *ChemSusChem* **2019**, *12*, 275–282.

[41] a) L. Ding, Y. Wei, Y. Wang, H. Chen, J. Caro, H. Wang, *Angew. Chem. Int. Ed.* **2017**, *56*, 1825–1829; *Angew. Chem.* **2017**, *129*, 1851–1855; b) K. Rasool, K. A. Mahmoud, D. J. Johnson, M. Helal, G. R. Berdiyorov, Y. Gogotsi, *Sci. Rep.* **2017**, *7*, 1598; c) L. Ding, Y. Wei, L. Li, T. Zhang, H. Wang, J. Xue, L.-X. Ding, S. Wang, J. Caro, Y. Gogotsi, *Nat. Commun.* **2018**, *9*, 155; d) B. Anasori, M. R. Lukatskaya, Y. Gogotsi, *Nat. Rev. Mater.* **2017**, *2*, 16098.

[42] R. Nair, H. Wu, P. Jayaram, I. Grigorieva, A. Geim, *Science* **2012**, *335*, 442–444.

[43] Y. You, V. Sahajwalla, M. Yoshimura, R. K. Joshi, *Nanoscale* **2016**, *8*, 117–119.

[44] D.-e. Jiang, V. R. Cooper, S. Dai, *Nano Lett.* **2009**, *9*, 4019–4024.

[45] H. W. Kim, H. W. Yoon, S.-M. Yoon, B. M. Yoo, B. K. Ahn, Y. H. Cho, H. J. Shin, H. Yang, U. Paik, S. Kwon, *Science* **2013**, *342*, 91–95.

[46] W. J. Koros, G. K. Fleming, *J. Membr. Sci.* **1993**, *83*, 1–80.

[47] S. Wang, Y. Wu, N. Zhang, G. He, Q. Xin, X. Wu, H. Wu, X. Cao, M. D. Guiver, Z. Jiang, *Energy Environ. Sci.* **2016**, *9*, 3107–3112.

[48] N. Yan, F. Capezzuto, M. Lavorgna, G. G. Buonocore, F. Tescione, H. Xia, L. Ambrosio, *Nanoscale* **2016**, *8*, 10783–10791.

[49] J. Yang, D. Gong, G. Li, G. Zeng, Q. Wang, Y. Zhang, G. Liu, P. Wu, E. Vovk, Z. Peng, *Adv. Mater.* **2018**, *30*, 1705775.

[50] S. Kim, J. Hou, Y. Wang, R. Ou, G. P. Simon, J. G. Seong, Y. M. Lee, H. Wang, *J. Mater. Chem. A* **2018**, *6*, 7668–7674.

[51] T. Rodenas, I. Luz, G. Prieto, B. Seoane, H. Miro, A. Corma, F. Kapteijn, F. X. L. i Xamena, J. Gascon, *Nat. Mater.* **2015**, *14*, 48.

[52] X. Wang, C. Chi, K. Zhang, Y. Qian, K. M. Gupta, Z. Kang, J. Jiang, D. Zhao, *Nat. Commun.* **2017**, *8*, 14460.

[53] Y. Hu, J. Wei, Y. Liang, H. Zhang, X. Zhang, W. Shen, H. Wang, *Angew. Chem. Int. Ed.* **2016**, *55*, 2048–2052; *Angew. Chem.* **2016**, *128*, 2088–2092.

[54] J. Hou, Y. Wei, S. Zhou, Y. Wang, H. Wang, *Chem. Eng. Sci.* **2018**, *182*, 180–188.

[55] D. Wang, Z. Wang, L. Wang, L. Hu, J. Jin, *Nanoscale* **2015**, *7*, 17649–17652.

[56] J. Shen, G. Liu, Y. Ji, Q. Liu, L. Cheng, K. Guan, M. Zhang, G. Liu, J. Xiong, J. Yang, *Adv. Funct. Mater.* **2018**, *28*, 1801511.

[57] P. Sun, M. Zhu, K. Wang, M. Zhong, J. Wei, D. Wu, Z. Xu, H. Zhu, *ACS Nano* **2013**, *7*, 428–437.

[58] R. Joshi, P. Carbone, F. C. Wang, V. G. Kravets, Y. Su, I. V. Grigorieva, H. Wu, A. K. Geim, R. R. Nair, *Science* **2014**, *343*, 752–754.

[59] M.-Y. Lim, Y.-S. Choi, J. Kim, K. Kim, H. Shin, J.-J. Kim, D. M. Shin, J.-C. Lee, *J. Membr. Sci.* **2017**, *521*, 1–9.

[60] J. Abraham, K. S. Vasu, C. D. Williams, K. Gopinadhan, Y. Su, C. T. Cherian, J. Dix, E. Prestat, S. J. Haigh, I. V. Grigorieva, *Nat. Nanotechnol.* **2017**, *12*, 546.

[61] H. Zhang, J. Hou, Y. Hu, P. Wang, R. Ou, L. Jiang, J. Z. Liu, B. D. Freeman, A. J. Hill, H. Wang, *Sci. Adv.* **2018**, *4*, eaaq0066.

[62] D. Li, Y. Yan, H. Wang, *Prog. Polym. Sci.* **2016**, *61*, 104–155.

[63] H. Liu, H. Wang, X. Zhang, *Adv. Mater.* **2015**, *27*, 249–254.

[64] L. Jin, Z. Wang, S. Zheng, B. Mi, *J. Membr. Sci.* **2018**, *545*, 11–18.